*Inorg. Chem.* **2005**, *44*, 5686–5695


# Unusual Syntheses, Structures, and Electronic Properties of Compounds Containing Ternary, T3-Type Supertetrahedral M/Sn/S Anions $[M_5Sn(\mu_3\text{-}S)_4(SnS_4)_4]^{10-}$ (M = Zn, Co)

**Christian Zimmermann,[†] Christopher E. Anson,[†] Florian Weigend,[‡] Rodolphe Clérac,[§] and Stefanie Dehnen*,[†]**

*Institut für Anorganische Chemie der Universität Karlsruhe (TH), Institut für Nanotechnologie, Forschungszentrum Karlsruhe GmbH, Germany, and Centre de Recherche Paul Pascal, CRPP−CNRS UPR 8641, 115 Avenue du Dr A. Schweitzer 33600 Pessac, France*

Received March 29, 2005

A recently discovered series of quaternary compounds of the general type $[K_m(ROH)_n][M_xSn_ySe_z]$ (R = H, Me), containing ternary anions with $[SnSe_4]^{4-}$-coordinated transition metal centers (M = Co, Mn, Zn, Cd, Hg) has now been extended by the synthesis and characterization of the two *ortho*-thiostannate-coordinated species, $[Na_{10}(H_2O)_{32}][M_5Sn(\mu_3\text{-}S)_4(SnS_4)_4]\cdot 2H_2O$ (M = Zn (**1**), Co (**2**)). The central structural motifs of compounds **1** and **2** are highly charged $[M_5Sn(\mu_3\text{-}S)_4(SnS_4)_4]^{10-}$ anions, being the first T3-type supertetrahedral *ternary* anions reported to date. The exposure of single crystals of **2** to a dynamic vacuum for several hours resulted in the reversible formation of a partially dehydrated, but still monocrystalline material of the composition $[Na_{10}(H_2O)_6][Co_5Sn(\mu_3\text{-}S)_4(SnS_4)_4]$ (**3**). The loss of 28 of the 34 water molecules only slightly affects the internal structure of the ternary anion in **3** and leads to a significant compacting of the crystal structure with closer linkage of the $[Co_5Sn_5S_{20}]^{10-}$ cluster units via the $Na^+$ cations. Magnetic measurements on **3** show that the ground state of the Co/Sn/S cluster is $S = 1/2$, indicating a significant antiferromagnetic coupling between the Co centers, which has also been rationalized by DFT investigations of the electronic situation in the ternary subunits of **1**–**3**.

## Introduction

The formation of compounds that contain ternary heavy atom M/E′/E frameworks, in which binary aggregates of main group elements $[E'_xE_y]^{q-}$ (E′ or E = group 13−15 or group 16) are stabilized by coordination to transition metal ions $M^{n+}$, is an area of increasing research activity.[1,2] This is the result both of their multifaceted structural variety and the interesting optoelectronic and magnetic properties of the resulting ternary or multinary compounds that in some cases combine the properties of the formally underlying binary phases.[3]

Compounds with group 15/16 binary fragments coordinating to transition metal centers, M, have usually been synthesized from salts of the binary anions of the respective group (15 or 16). In contrast, most of the known compounds with elemental combinations M/14/16 or M/13/16 have been prepared using separate sources for the M, E′, and E atoms. Recent examples include clusters, such as $[Cu_{11}In_{15}Se_{16}(SePh)_{24}(PPh_3)_4]$,[4] phases containing ligand-free Cd/In/S anions,[5] such as $[Cd_{16}In_{64}S_{134}]^{44-}$,[5c] and solids, such as $A_2[MnGe_4S_{10}]\cdot nH_2O$ (A = $C_6H_{14}N_2$, Rb, Cs; $n$ = 0, 2, 3),[6] $A_2[Hg_3E'_2S_8]$ (A = K, Rb; E′ = Ge, Sn),[7] and $[Mn_2\{H_2N(CH_2)_2NH_2\}Sb_2S_5]$.[8]

* To whom correspondence should be addressed. E-mail: dehnen@aoc.uka.de. Phone: int + 49/721-608-2850. Fax: int + 49/721-608-7021.
† Institut für Anorganische Chemie der Universität Karlsruhe.
‡ Institut für Nanotechnologie.
§ Centre de Recherche Paul Pascal.

(1) Feng, P.; Bu, X.; Zheng, N. *Acc. Chem. Res.* **2005**, *38*, 293−303. (b) Bu, X.; Zheng, N.; Feng, P. *Chem.−Eur. J.* **2004**, *10*, 3356−3362. (c) Kanatzidis, M. G.; Sutorik, A. C. *Prog. Inorg. Chem.* **1995**, *43*, 151−265.
(2) (a) Wachter, J. *Angew. Chem., Int. Ed.* **1998**, *37*, 750−768. (b) Drake, G. W.; Kolis, J. W. *Coord. Chem. Rev.* **1994**, *137*, 131−178.
(3) Solymar, L.; Walsh, D. *Electrical Properties of Materials*, 6th ed.; Oxford University Press: New York, 1998.
(4) Eichhöfer, A.; Fenske, D. *J. Chem. Soc., Dalton Trans.* **2000**, 941−944.
(5) (a) Li, H.; Kim, J.; Groy, T. L.; O'Keeffe, M.; Yaghi, O. M. *J. Am. Chem. Soc.* **2001**, *123*, 4867−4868. (b) Su, W.-P.; Huang, X.-Y.; Li, J.; Fu, H.-X. *J. Am. Chem. Soc.* **2002**, *124*, 12944−12945. (c) Li, H.; Kim, J.; O'Keeffe, M.; Yaghi, O. M. *Angew. Chem., Int Ed.* **2003**, *42*, 1819−1821.
(6) (a) Cahill, C. L.; Parise, J. B. *Chem. Mater.* **1997**, *9*, 807−811. (b) Loose, A.; Sheldrick, W. S. *Z. Naturforsch.* **1997**, *52b*, 687−692.



10.1021/ic050466o CCC: $30.25 
Published on Web 07/13/2005

However, the syntheses of $(Me_4N)_2[Mn_2Ge_4S_{10}]$ from $(Me_4N)_4[Ge_4S_{10}]$,[9] that of $K_2[HgSnTe_4]$[10] from $K_4[SnTe_4]$, and the recently reported formation of mesoporous phases, such as $(CP)_x[Pt_yE'_4E_{10}]$ (CP = cetylpyridinium, E′ = Ge, Sn; E = S, Se; $x = 1.9-2.8$; $y = 0.9-1.6$)[11] and $(CTA)_2[M_2Ge_4S_{10}]$ (M = Co, Ni, Zn),[12] demonstrated the synthetic potential of group 14/16 binary anions in reactions toward transition metal salts. The elemental combinations and structures of these phases result in narrow band gaps or intense photoluminescence; and such compounds have therefore been considered potentially suitable for optoelectronic, photosynthetic, or photocatalytic applications.[11]

In the course of our investigations of the reactivity and coordination chemistry of chalcogenostannate anions, we recently described the synthesis of a series of novel complexes featuring discrete ternary anions of the general type $[M_4(\mu_4\text{-Se})(SnSe_4)_4]^{10-}$ (M = Co, Mn, Zn, Cd, Hg),[13] being the first molecular M/Sn/Se complexes to be free of covalently bound ligands. The coordination oligomers were stabilized, exclusively, through coordinative interactions with different complex counterion aggregates. These anionic substructures were the first to show the desired transfer of intact $[SnSe_4]^{4-}$ ions into the coordination sphere of transition metal ions. Recently, a series of solvent-free sulfur analogues, $K_{10}[M_4(\mu_4\text{-S})(SnS_4)_4]$ (M = Mn, Fe, Co, Zn), was also reported; they were, however, prepared differently employing a potassium−polysulfide flux.[14]

The investigations on the $[SnE_4]^{4-}$ anions are now extended by the use of the lighter homologous salt $Na_4[SnS_4]$. Here, we present the syntheses and crystal structures of the novel compounds $[Na_{10}(H_2O)_{32}][M_5Sn(\mu_3\text{-S})_4(SnS_4)_4]\cdot 2H_2O$ (M = Zn (**1**), Co (**2**)) and the partial dehydration product of **2**, $[Na_{10}(H_2O)_6][Co_5Sn(\mu_3\text{-S})_4(SnS_4)_4]$ (**3**). The molecular charge of the anions, which necessitates the statistical distribution of five M atoms and one Sn atom over six atomic positions within the anions, was determined from the ten $Na^+$ ions in all three X-ray structures and is in agreement with the chemical analyses, the quantumchemical investigations using density functional (DFT) methods, and the magnetic behavior of the open-shell Co compounds. The latter was investigated by magnetic measurements of a polycrystalline sample of compound **3**. These show evidence for a significant antiferromagnetic coupling between the $\mu_3$-S-bridged $Co^{II}$ centers, which was confirmed by analyses of the spin density calculated for the Co/Sn/S anion.

## Experimental Methods

**Starting Materials.** $ZnX_2$ (X = Cl, Br) were purchased from Merck, and $[Co(en)_3]X_3$ (*en* = 1,2-diaminoethane; X = Cl, Br) were prepared according to literature procedures.[15a] $Na_4[SnS_4]$ was prepared by a method similar to that previously described;[15b] an alternative method to provide a suitable aqueous solution of $Na_4[SnS_4]$ has been the in situ reaction of stoichiometric amounts of $SnCl_4$ and $Na_2S$ in water.[15c] All synthesis steps were performed with strong exclusion of air and external moisture ($N_2$ atmosphere on a high-vacuum, double-manifold Schlenk line or Ar atmosphere in a glovebox). THF was dried and freshly distilled prior to use; the water was degassed. $^{119}Sn$ NMR data for $Na[SnS_4]$ in $D_2O$ were from (a) a saturated solution (68.9 ppm (s)) and (b) a solution with a concentration of $<10^{-3}$ mol $L^{-1}$ (73.7 ppm (s)).

**Synthesis of $[Na_{10}(H_2O)_{32}][Zn_5Sn(\mu_3\text{-S})_4(SnS_4)_4]\cdot 2H_2O$ (1).** $ZnCl_2$ (0.066 g, 0.50 mmol) was added to a solution of 0.170 g (0.50 mmol) of $Na_4[SnS_4]$ in 14 mL of $H_2O$. After the mixture was stirred for 4 h, the colorless solution was layered with 10 mL of THF. Compound **1** crystallized as colorless needles, over the course of 2 days. Isolation by decanting the mother liquor and the loose precipitate and drying compound **1** leads to partial dehydration, as observed for compound **2** (vide infra). In contrast to **2**, such dehydration always resulted in X-ray amorphous material with differing $H_2O$ content as determined from elemental analysis. Yield: 0.119 g (0.050 mmol, 50% based on Zn).

**Synthesis of $[Na_{10}(H_2O)_{32}][Co_5Sn(\mu_3\text{-S})_4(SnS_4)_4]\cdot 2H_2O$ (2).**[16] $[Co(en)_3]Cl_3$ (0.160 g, 0.46 mmol) or $[Co(en)_3]Br_3$ (0.220 g, 0.46 mmol) was added to a solution of 0.170 g (0.50 mmol) of $Na_4[SnS_4]$ in 14 mL of $H_2O$; upon the addition, the reaction mixture immediately turned dark brown. After the mixture was stirred for 12 h, an insoluble black precipitate, containing CoS and S, was removed by filtration. The remaining solution was layered with 14 mL of THF. Over the course of 2 days, the solution became lighter in color upon crystallization of black blocks of **2** together with further black precipitate, presumably further amounts of CoS and


(7) Liao, J.-L.; Marking, G. M.; Hsu, K. F.; Matsushita, Y.; Ewbank, M. D.; Borwick, R.; Cunningham, P.; Rosker, M. J.; Kanatzidis, M. G. *J. Am. Chem. Soc.* **2003**, *125*, 9484−9493.

(8) Schur, M.; Bensch, W. *Z. Naturforsch.* **2002**, *57b*, 1−7.

(9) Yaghi, O. M.; Sun, Z.; Richardson, D. A.; Groy, T. L. *J. Am. Chem. Soc.* **1994**, *116*, 807−808.

(10) Dhingra, S. S.; Haushalter, R. C. *Chem. Mater.* **1994**, *6*, 2376−2381.

(11) Trikalitis, P. N.; Rangan, K. K.; Kanatzidis, M. G. *J. Am. Chem. Soc.* **2002**, *124*, 2604−2613.

(12) McLachlan, M. J.; Coombs, N.; Ozin, G. A. *Nature* **1999**, *397*, 681−684.

(13) (a) Zimmermann, C.; Melullis, M.; Dehnen, S. *Angew. Chem., Int. Ed.* **2002**, *41*, 4269−4272. (b) Dehnen, S.; Brandmayer, M. K. *J. Am. Chem. Soc.* **2003**, *125*, 6618−6619. (c) Melullis, M.; Zimmermann, C.; Anson, C. E.; Dehnen, S. *Z. Anorg. Allg. Chem.* **2003**, *629*, 2325−2329. (d) Brandmayer, M. K.; Clérac, R.; Weigend, F.; Dehnen, S. *Chem.—Eur. J.* **2004**, *10*, 5147−5157.

(14) (a) Palchik, O.; Iyer, R. G.; Canlas, C. G.; Weliky, D. P.; Kanatzidis, M. G. *Z. Anorg. Allg. Chem.* **2004**, *630*, 2237−2247. (b) Palchik, O.; Iyer, R. G.; Liao, J. H.; Kanatzidis, M. G. *Inorg. Chem.* **2003**, *42*, 5052−5054.

(15) (a) *Gmelins Handbuch der Anorganischen Chemie*; Verlag Chemie GmbH: Weinheim, Germany 1964; 8. Aufl., Kobalt B. (b) Eisenmann, B.; Hansa, J. *Z. Kristallogr.* **1993**, *203*, 299−300. (c) Schiwy, W.; Pohl, S.; Krebs, B. *Z. Anorg. Allg. Chem.* **1973**, *402*, 77−86.


(16) Compounds with ternary Co/Sn/S anions can only be isolated when the reactivity of the $Co^{2+}$ or $Co^{3+}$ ion is reduced by coordinating ligands; *en* complexes are be suitable starting materials for this purpose because they are water soluble and the ligands allow for a controlled reaction but finally leave the coordination sphere upon reaction with $[SnS_4]^{4-}$. The synthesis of compound **2** can also be carried out using $[Co(en)_2X_2]X$ (X = Cl, Br); however, the product shows higher crystallinity when the reaction is performed as described. This probably results from a slower reaction rate caused by the presence of an additional chelating *en* ligand to be removed during formation of **2**. In contrast, reactions of $CoX_2$ (X = Cl, Br) with $[SnS_4]^{4-}$ anions lead to quantitative formation of CoS. Complexation of these salts by multidentate polyamines (such as *tetren*, $C_8H_{23}N_5$) help to control the reaction to produce **2**, as well, but the yields are lower than those produced via the described route. Reactions of other transition metal salts or complexes with $Na_4[SnS_4]$ produce appropriately colored solutions in some cases (e.g., with $Mn^{2+}$, $Cd^{2+}$, $Hg^{2+}$) but do not yield crystalline products, which may be the result of the (larger) ionic radii to the $[SnS_4]^{4-}$ ion leading to an anion too large to crystallize with $Na^+$ counterions in the present structure type. Reactions with suitably sized ions (e.g., $Cu^+$, $Fe^{3+}$), however, lead to redox processes under the given reaction conditions. Variations of both the reaction conditions and the starting materials that allow the formation of stable ternary networks containing further transition metal ions are the focus of our current work.

S. Yield: 0.132 or 0.157 g (0.056 or 0.066 mmol, 61% or 72% based on Co used as $[Co(en)_3]Br_3$ or $[Co(en)_3]Cl_3$, respectively). As observed with **1**, drying of isolated crystals causes loss of water molecules. The dehydration product of **2** with 28 fewer water molecules per formula unit is still crystalline and is therefore discussed separately (compound **3**).

**Synthesis of $[Na_{10}(H_2O)_6][Co_5Sn(\mu_3\text{-}S)_4(SnS_4)_4]$ (3).** The single crystals of a complete batch of **2** were isolated by decanting both the mother liquor and the loose byproduct precipitate, and the washing procedure was repeated with a THF/$H_2O$ (1/1) mixture. The solid material (0.157 g) was then pumped with dynamic vacuum for 5 h. The crystals changed appearance, compared to that of the starting material, **2**; a metallic luster appeared, and cracking of the crystal surfaces was observed. The yield is quantitative with respect to **2**. The majority of the partially dehydrated crystals were suitable for X-ray structure determination. Although some of the individual crystals tested showed poor quality, determination of the lattice parameters was possible in all cases; therefore, the yield is assumed to be quantitative with respect to **2**. A reversal of the partial dehydration process is possible by addition of a droplet of water (0.02 mL) to a sample of **3**, regenerating single crystals of **2**.

**NMR Spectroscopy.** $^{119}$Sn NMR data were recorded using a Bruker AVANCE 400 MHz spectrometer at a frequency of 142.21 MHz.

**Elemental Analyses.** From elemental analyses of partially dried (i.e., partially dehydrated) samples of **1** and **2**, the ratios of the elements are as follows (referring to weight %): Na/Zn/Sn/S as 1/1.43/2.57/2.76 (**1**) and Na/Co/Sn/S as 1/1.28/2.57/2.74 (**2**). The calculated ratios for $Na_{10}M_5Sn_5S_{20}{\cdot}n(H_2O)$ are 1/1.42/2.58/2.79 (M = Zn, **1**) and 1/1.28/2.58/2.79 (M = Co, **2**), in excellent agreement with the experimentally observed data. Details of the analytical procedures are available from www.ianz.govt.nz.

**X-ray Diffractometry.** X-ray data were collected on a Bruker SMART Apex CCD diffractometer using graphite-monochromated Mo K$\alpha$ radiation ($\lambda = 0.71073$ Å) at $T = 200$ K. Structure solution by direct methods and full-matrix least-squares refinement against $F^2$ were carried out using the SHELXTL software package.[17a] The non-hydrogen atoms were anisotropically refined; H atoms on the water O atoms were not included. Initially the six metal centers in the central octahedron, M(1−6) (M = Co, Zn), were assigned as the respective metal, with the four outer tin sites refined as Sn. This resulted in significantly lower temperature factors for M(1−6) compared to that of the other atoms in the clusters. As discussed in more detail below, the six "metal" sites were each refined, following the full elemental analysis for **2** which indicated a Co/Sn molar ratio of 5/5, with composition {5/6M + 1/6Sn}, modeling a statistical disorder of 1 Sn atom and 5 M atoms over these six apparently equal positions. This resulted in thermal parameters consistent with the other atoms, and no attempt was made to vary the occupancies between the atoms or to refine the four outer Sn sites with slight admixtures of Co or Zn.

Two (in **1** and **2**) or three (in **3**) Na atoms show 2-fold disorder, and several O atoms show 2-fold (in **1**−**3**) or 3-fold (in **1**) disorder; in **1** and **2**, one Na atom has an 0.5 site occupancy. Most of these disordered atoms were successfully refined anisotropically, although a few Na (**3**) and O atoms (**2** and **3**) were refined isotropically. Further details of the single-crystal X-ray diffractometry are summarized in Table 1 and ref 17b.

**Optical Absorption Spectroscopy.** Single crystals of **1** and **2** were transferred into a droplet of Nujol oil between two quartz plates and pulverized. The resulting suspension was investigated by means of a Perkin-Elmer Lambda 900 UV/Vis/NIR spectrometer between 250 and 1100 nm.

**Magnetic Measurements.** The magnetic susceptibility measurements were obtained using a Quantum Design Squid magnetometer MPMS-XL. The samples of **3** were prepared in a glovebox under an argon atmosphere and packed in a sealed plastic bag. The raw data were corrected for the sample holder and the orbital diamagnetic contributions calculated from Pascal's constants.[18] The sample has been systematically checked for ferromagnetic impurities, which were found to be absent by measuring the field dependence of the magnetization at $T = 100$ K and the temperature dependence of the dc susceptibility at $H = 1000$ and 10 000 Oe. Temperature-independent paramagnetism (TIP) was systematically observed and removed in all samples. The estimation of the TIP was determined experimentally by consideration of the residual $S = 1/2$ Curie paramagnetism which should be a plateau in the $\chi T$ versus $T$ plot. The observed TIP values range from 0.9 to 1.4 $\times$ $10^{-6}$ emu $g^{-1}$ of Co (1.6 to 2.5 $\times$ $10^{-3}$ emu $mol^{-1}$ of Co) on the seven different batches of **3** measured.

**Theoretical Methods.** Density functional (DFT) calculations[19] were performed using the program system Turbomole[20] (Ridft program,[21] Becke−Perdew functional (BP86),[22] basis sets of TZVP

(17) (a) Sheldrick, G. M. *SHELXTL*, version 5.1; Bruker AXS Inc.: Madison, 1997. (b) The observed disorder in compounds **1** and **2** can be described as follows: Na(8) and Na(9) lie on inversion centers, and each appeared at first to be surrounded by four further Na cations, Na(11), Na(11′), Na(13), and Na(13′) about Na(8), and Na(12), Na(12′), Na(14), and Na(14′) about Na(9). These were then apparently bridged by ($\mu_3$-OH) ligands, O(28) and O(29) and O(32) and O(33), respectively. However, the thermal parameters for Na(11) to Na(14) were too high if they were refined with unit occupancy, and attempts to refine the four oxygen atoms anisotropically resulted in unreasonable thermal parameters. However, if Na(11) to Na(14) were refined at half occupancy, their temperature factors came into line with the ordered sodium centers in the structure. Furthermore, the four oxygen sites could readily each be split into a pair of adjacent half atoms, which could also then be refined normally, in each case, one bridging to one-half of a sodium atom (e.g., Na(11)) and the other bridging to the other sodium of the disorder pair (e.g., Na(12)), both with normal geometries. We thus assign each of the cationic units centered at Na(8) and Na(9) as 2-fold disordered $[Na_3(\mu\text{-}OH_2)_4]^{3+}$ units. Note that if the sodium atoms are all refined with full occupancies (i.e., assuming no disorder), the geometries at the oxygen atoms become such that it is necessary to assign them as triple-bridging hydroxo ligands, and the units as $[Na_5(\mu_3\text{-}OH)_4]^+$. The overall effect is the reduction of the positive charge available; it does not increase it. Similarly, it was found that refinement of Na(10) and its coordinated waters with unit occupancy was unsatisfactory, but that Na(10) could be successfully refined at half occupancy, together with an adjacent one-half of an oxygen atom (O(34A) in the cif file), which made normal hydrogen-bonding distances to adjacent ordered oxygen atoms possible, while the oxygen atoms coordinated to Na(10) could all be split and refined as pairs of one-half of an oxygen. It was found that the disorder at these three sites was correlated; the disordered oxygen atoms labeled *A* in the cif file, together with Na(11) and Na(12), form one set of atoms that made sensible nonbonding contacts, while the oxygen atoms labeled *B* in the cif file, with Na(10), Na(13), and Na(14), formed a second mutually consistent set. Two further oxygen atoms, O(5), O(19), O(23), and O(26), were also disordered, but without correlating to either of the two above sets of atoms.

(18) *Theory and Applications of Molecular Paramagnetism*; Boudreaux, E. A., Mulay, L. N., Eds.; John Wiley & Sons: New York, 1976.

(19) (a) Parr, R. G.; Yang, W. *Density Functional Theory of Atoms and Molecules*; Oxford University Press: New York, 1988. (b) Ziegler, T. *Chem. Rev.* **1991**, *91*, 651−667.

(20) (a) Ahlrichs, R.; Bär, M.; Häser, M.; Horn, H.; Kölmel, C. *Chem. Phys. Lett.* **1989**, *162*, 165−169. (b) Treutler, O.; Ahlrichs, R. *J. Chem. Phys.* **1995**, *102*, 346−354. (c) von Arnim, M.; Ahlrichs, R. *J. Chem. Phys.* **1999**, *111*, 9183−9190.

(21) (a) Eichkorn, K.; Treutler, O.; Öhm, H.; Häser, M.; Ahlrichs, R. *Chem. Phys. Lett.* **1995**, *242*, 652−660. (b) Eichkorn, K.; Weigend, F.; Treutler, O.; Ahlrichs, R. *Theor. Chim. Acta* **1997**, *97*, 119−124.

**Table 1.** Crystallographic and Refinement Details of **1**−**3** at 203 K

| | **1** | **2** | **3** |
|---|---|---|---|
| empirical formula | $H_{68}O_{34}Zn_5Na_{10}S_{20}Sn_5$ | $H_{68}O_{34}Co_5Na_{10}S_{20}Sn_5$ | $H_{12}O_6Co_5Na_{10}S_{20}Sn_5$ |
| fw (g mol$^{-1}$) | 2403.94 | 2371.74 | 1867.30 |
| cryst color and shape | colorless needle | black block | black block |
| cryst size | 0.13 × 0.17 × 0.22 | 0.15 × 0.08 × 0.20 | 0.12 × 0.15 × 0.22 |
| cryst syst | triclinic | triclinic | triclinic |
| space group | $P\bar{1}$ (No. 2) | $P\bar{1}$ (No. 2) | $P\bar{1}$ (No. 2) |
| $a$ (Å) | 14.8457(10) | 14.712(2) | 13.436(2) |
| $b$ (Å) | 14.8772(9) | 14.737(2) | 13.570(2) |
| $c$ (Å) | 17.5101(11) | 17.142(2) | 14.105(2) |
| α (deg) | 97.402(1) | 97.298(2) | 95.770(3) |
| $\beta$ (deg) | 100.211(1) | 99.264(2) | 117.889(3) |
| $\gamma$ (deg) | 103.956(1) | 103.868(3) | 98.364(3) |
| $V$ (Å$^3$) | 3633.6(4) | 3507.5(8) | 2206.7(6) |
| $Z$ | 2 | 2 | 2 |
| $\rho_{calc}$ (g cm$^{-3}$) | 2.197 | 2.185 | 2.810 |
| $\mu$(Mo Kα) (mm$^{-1}$) | 4.007 | 3.504 | 5.674 |
| 2$\theta$ range (deg) | 3−56 | 3−56 | 4−55 |
| abs correction type | multiscan (SADABS) | multiscan (SADABS) | multiscan (SADABS) |
| $T_{min}/T_{max}$ | 0.557/0.831 | 0.361/0.801 | 0.550/0.831 |
| no. of measured reflns | 18078 | 17136 | 8187 |
| no. of independent reflns | 15329 | 14651 | 7622 |
| $R$(int) | 0.0404 | 0.0444 | 0.0256 |
| no. of independent reflns with $I > 2\sigma(I)$ | 11168 | 8867 | 4912 |
| no. of parameters | 827 | 686 | 450 |
| wR2 (all data) | 0.1593 | 0.1819 | 0.1822 |
| $S$ (all data) | 1.003 | 1.028 | 1.069 |
| R1 ($I > 2\sigma(I)$) | 0.0551 | 0.0625 | 0.0676 |
| largest difference peak/hole [e$^-$ Å$^{-3}$] | 1.358/−1.484 | 1.718/−1.207 | 2.811/−1.278 |
| CSD number | 415235 | 415234 | 415219 |

**Scheme 1.** Synthesis of **1**

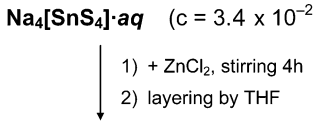


**Scheme 2.** Synthesis of **2** and **3**

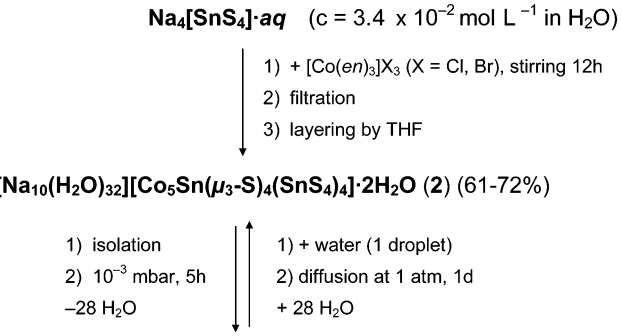


quality,[21b] relativistic effective core potentials[23] (ECP) for the inner 46 electrons of Sn). Both compensation of the negative charges of the calculated molecules and simulation of the charges of the two H atoms per cluster unit were achieved by employing the Cosmo model,[23] which has previously turned out to be suitable for these purposes.[13] Calculations were performed without symmetry restrictions ($C_1$ symmetry); therefore, convergence into local minimum structures can be expected.

## Results and Discussion

**Synthesis.** The synthesis of **1**, $[Na_{10}(H_2O)_{32}][Zn_5Sn(\mu_3\text{-}S)_4(SnS_4)_4]\cdot 2H_2O$, from $Na_4[SnS_4]$ and $ZnCl_2$ is summarized in Scheme 1. Scheme 2 shows the reaction of $Na_4[SnS_4]$ with $[Co(en)_3]X_3$ (X = Cl, Br) in water that yields compound **2**, $[Na_{10}(H_2O)_{32}][Co_5Sn(\mu_3\text{-}S)_4(SnS_4)_4]\cdot 2H_2O$,[16] and the reversible dehydration of **2** to give compound **3**, $[Na_{10}(H_2O)_6][Co_5Sn(\mu_3\text{-}S)_4(SnS_4)_4]$. The observation of elemental sulfur occurring in the synthesis of **2** is consistent with the reduction of the $Co^{III}$ centers by $S^{2-}$ anions. The latter were available for the reduction as well as for the formation of compounds **1** and **2**, resulting from partial dimerization of $[SnS_4]^{4-}$ anions to give $[Sn_2S_6]^{2-}$ and $S^{2-}$, as previously observed for the $[SnSe_4]^{4-}$ homologues.[13]

Compounds **1**−**3** are ionic compounds that contain the complex ternary anions $[M_5Sn(\mu_3\text{-}S)_4(SnS_4)_4]^{10-}$ (M = Zn, Co) together with 10 $Na^+$ ions as determined by X-ray diffractometry on all three compounds. The accuracy of this formulation was confirmed by elemental analysis of samples of partially dehydrated compound **2** and is further underlined by only small deviations between the structural data from the DFT optimizations of the anionic $[M_5Sn_5S_{20}]^{10-}$ units and the experimental values (vide infra).

The compositions of **1**−**3** show that the $[SnS_4]^{4-}$ anions of the starting material have acted as ligands, as $S^{2-}$ donors, and as a source for $Sn^{IV}$ centers. Reactions using $K_4[SnSe_4]$ usually produce crystals of $[K_4(MeOH)_4][Sn_2Se_6]$ as coproducts, whereas a compound like $Na_4[Sn_2S_6]$ did not precipitate during the synthesis of **1** or **2**. However, traces of elemental sulfur that precipitated during the preparation of **2** on the glass wall of the Schlenk tube indicated the occurrence of

(22) (a) Becke, A. D. *Phys. Rev. A* **1988**, *38*, 3098−3109. (b) Vosko, S. H.; Wilk, L.; Nusair, M. *Can. J. Phys.* **1980**, *58*, 1200−1205. (c) Perdew, J. P. *Phys. Rev. B* **1986**, *33*, 8822−8837.
(23) Dolg, M.; Stoll, H.; Savin, A.; Preuss, H. *Theor. Chim. Acta* **1989**, *75*, 173−194.

**Table 2.** Distances (Å) and Angles (deg) of Ternary Anions and Counterion Aggregates in **1**−**3**[a]

| | **1** (Zn/Sn) | **2** (Co/Sn) | **3** (Co/Sn) |
|---|---|---|---|
| Sn−$S_{term}$ | 2.3531(16)−2.3632(17) | 2.343(3)−2.358(3) | 2.349(5)−2.363(4) |
| Sn−($\mu$-S) | 2.3964(17)−2.4152(16) | 2.381(3)−2.398(3) | 2.412(4)−2.447(4) |
| M−($\mu$-S) | 2.3533(16)−2.3970(16) | 2.302(3)−2.352(3) | 2.318(5)−2.357(4) |
| M−($\mu_3$-S) | 2.3241(17)−2.3494(18) | 2.281(3)−2.299(3) | 2.320(4)−2.349(4) |
| M···M ($O_h$ edges) | 3.706(2)−3.755(2) | 3.628(4)−3.685(3) | 3.706(5)−3.755(5) |
| $S_{term}$−Sn−($\mu$-S) | 105.23(6)−109.96(6) | 105.87(9)−110.18(11) | 106.33(15)−112.9(2) |
| ($\mu$-S)−Sn−($\mu$-S) | 109.38(6)−111.96(6) | 108.59(9)−111.69(9) | 106.26(15)−111.79(15) |
| ($\mu$-S)−M−($\mu$-S) | 101.54(6)−103.65(6) | 100.20(10)−103.13(10) | 102.78(16)−105.03(17) |
| ($\mu$-S)−M−($\mu_3$-S) | 108.43(6)−110.38(6) | 108.89(10)−110.90(10) | 106.81(16)−111.65(16) |
| ($\mu_3$-S)−M−($\mu_3$-S) | 114.78(6)−116.49(6) | 113.73(10)−115.69(11) | 113.19(15)−116.03(15) |
| M−($\mu$-S)−Sn | 103.22(7)−105.45(6) | 103.13(11)−105.68(10) | 105.40(16)−107.81(18) |
| M−($\mu_3$-S)−M | 104.73(6)−106.49(6) | 104.82(11)−107.18(11) | 105.30(16)−107.93(18) |
| | distances within the counterion aggregate | | |
| Na···S | 2.843(2)−3.047(4) | 2.793(16)−3.024(5) | 2.75(4)−3.24(5) |
| Na···O | 2.343(9)−2.865(15) | 2.291(18)−2.83 (4) | 2.33(5)−2.73(6) |

[a] M = Zn or Sn for **1** and M= Co or Sn for **2** and **3** in the case of the six core atoms.

the $2Co^{III} + S^{2-} \rightarrow S + 2Co^{II}$ redox reaction. This is consistent with the assumption of formal oxidation states $Co^{II}$, $Sn^{IV}$, and $S^{2-}$ in the ternary anions in **2** and **3**, and the analogous reaction has been observed in related reactions of $[SnSe_4]^{4-}$ anions. The standard redox potentials in basic solution (pH ≈ 12 for $10^{-3}$ mol $L^{-1}$ $[SnS_4]^{4-}$) also indicate that the $[Co^{III}(en)_3]^{3+} \rightarrow [Co^{II}(en)_3]^{2+}$ process should take place ($E^0_{1/2} = -0.18$ V;[25a] $S^{2-} \rightarrow 1/8S_8$, $E^0_{1/2} = -0.48$ V.[25b]

**Crystal Structures.** Compound **1** forms very small colorless needles. Compound **2** crystallizes as black blocks that are brownish in thin layers. The material is very air-sensitive and decomposes upon redissolution in $H_2O$. However, crystals of **2** could be isolated without decomposition by rapid transfer into polyfluoroether oil for the X-ray investigation. Attempts to isolate dry material by washing away the coprecipitating byproducts (see Experimental Methods) with a water/THF (1/1) mixture and then removing the residual solvent leads to partial dehydration of **2** resulting in the formation of black single crystals of **3**.

The central structural motif of **1**−**3** is purely inorganic discrete ternary anions of $[M_5Sn(\mu_3\text{-}S)_4(SnS_4)_4]^{10-}$ that are embedded in a coordination sphere of solvated $Na^+$ ions. Because the structural parameters of the ternary anions in **1**−**3** differ only slightly, the structure of the anion in **1** is shown as an example in Figure 1; the same numbering scheme is used for all three clusters. Table 2 summarizes structural parameters of the anions and the embedding counterion aggregate.

In the ternary anions of **1**−**3**, five zinc or cobalt centers that form a square pyramid and one additional tin atom are arranged in a slightly distorted octahedral manner, being linked by four $\mu_3$-bridging sulfur ligands at four Δ-(M, Sn) faces to form an inner adamantane-type $M_5SnS_4$ cage (bold black lines in Figure 1). Four $[SnS_4]^{4-}$ units cap the remaining four Δ-(M, Sn)$_3$ faces of the $M_5Sn$ octahedron so that four further adamantane-type cages result, two of which have the composition $[M_3SnS_6]$ and two are $[M_2Sn_2S_6]$; each of the outer Sn atoms is additionally coordinated by one terminal sulfur ligand. The latter define the corners of a T3-type supertetrahedron with S···S edge distances of 11.316(2)−11.477(3) (**1**), 11.180(5)−11.384(5) (**2**), and 11.360(7)−11.564(9) Å (**3**). However, a slight deviation from tetrahedral geometry is observed, which is reflected by the variation of bond lengths around mean values (to a maximum of ±0.022, ±0.034, and ±0.018 Å in **1**, **2**, and **3**, respectively) and by the observed ranges of angles (maximum differences of respective angles of 4.73° in **1**, 4.30° in **2**, and 6.67° in **3**).

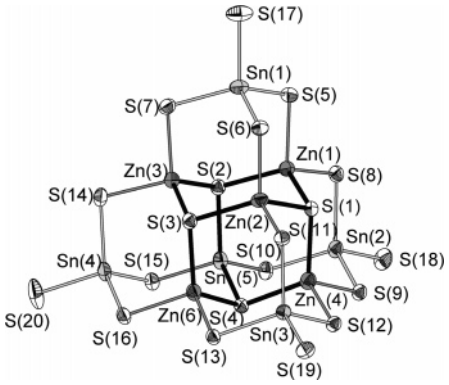


**Figure 1.** Fifty percent probability thermal ellipsoid plot of the ternary anion in **1**. Note that the positions of M atoms (Zn in **1**, shown here; Co in **2**) and Sn(5) are statistically occupied in a 5/1 ratio; each of these six sites was refined as a superposition of M (sof = 0.833) and Sn (sof = 0.167).

It was not possible to determine the position of the extra Sn atom within the inner $M_5Sn$ fragment. Neither distinct differences in the metal-sulfide distances nor an irregularity of the thermal ellipsoids pointed to a definite Sn position, which indicates an even statistical distribution of the Sn atom over the corners of the octahedron. However, only by considering a partial occupation of Sn on the Co sites (1/6 vs 5/6) was it possible to bring the values of the respective thermal parameters into line with those of the other heavy atoms within the cluster anion. Whereas the presence of these "inner" Sn atoms in **1**−**3** can be considered certain, their origin is still unclear. It is known that $[SnS_4]^{4-}$ anions can undergo hydrolysis in an aqueous solution to form complexes

(24) (a) Klamt, A. *J. Chem. Phys.* **1995**, *103*, 9312−9320. (b) Schäfer, A.; Klamt, A.; Sattel, D.; Lohrenz, J. C. W.; Eckert, F. *Phys. Chem. Chem. Phys.* **2000**, *2*, 2187−2193.

(25) (a) Huheey, J. E.; Keiter, E. A.; Keiter, R. L. *Anorganische Chemie: Prinzipien von Struktur und Reaktivität*, 2nd ed.; de Gruyter: Berlin, 1995; p 477. (b) Hollemann, A. F.; Wiberg, N. *Lehrbuch der Anorganischen Chemie*, 100th ed.; de Gruyter: Berlin, 1985; p 543. (c) Hollemann, A. F.; Wiberg, N. *Lehrbuch der Anorganischen Chemie*, 100th ed.; de Gruyter: Berlin, 1985; p 800.

such as $[SnS_2(SH)_2(OH)_2]^{4-}$ [25c] which might transform by ligand exchange into sulfur-free Sn anion complexes. Another possibility would be the formation of a larger thiostannate aggregate of the yet unprecedented $[Sn_3S_{10}]^{8-}$ type (which can be viewed as an $[SnS_3]^{2-}$ adduct of an $[Sn_2S_7]^{6-}$ anion or as a fragment of a $[SnS_3]^{2-}$ polymeric chain)[26] and its coordination to a hypothetically preformed $[Zn_5(\mu_3\text{-}S)_2(SnS_4)_2]^{2-}$ unit.

It appears that the observation of this species, instead of a $[Co_6Sn_4S_{20}]^{12-}$ cluster anion stabilized by 12 $Na^+$ ions, is a result of the packing requirements for a given type of cation; because of its size, this ternary anion fits perfectly in the environment of 10 octahedrally coordinated $Na^+$ ions, whereas a twelve-fold charge could not be compensated because of lack of space. Thus, the distinct steric demand of the counterion environment results in the crystallization of the observed type of anion, at the same time ruling out the embedding of a different structure which has previously been observed in the presence of $K^+$ ions. The other type of discrete ternary anions that have been obtained, so far, by reacting either $K_4[SnSe_4]$ or a mixture of $K_2S/Sn/S$ with transition metal compounds, $[M_4Sn_4E_{17}]^{10-}$,[13,14] not only show another composition but also adopt another molecular structure, which is based on four linked barrelane-type cages (P1 supertetrahedron). The nature of the alkali metal ion, together with its preferred coordination environment, seems to be the key parameter in controlling the observed cluster structure.

The T3 anionic cluster structure represents the topological equivalent of a section of the Sphalerite-type structure. This is also the case for the larger supertetrahedral Cd/In/S clusters of the Tn family, such as $[Cd_4In_{16}S_{35}]^{14-}$ (T4) or $[Cd_{16}In_{64}S_{134}]^{44-}$ (T2 arrangement of T4 clusters),[5] and some T3 chalcogenido or pnictido-bridged binary $d^{10}$-metal clusters, $[M^{II}_{10}(\mu_3\text{-}E)_4(\mu\text{-}EPh)_{12}L_4]$ ($M^{II}$ = Zn, E = Te, L = P*n*Pr$_3$;[27] $M^{II}$ = Cd, E = Se, L = $PPh_3$[28]), $[In_{10}(\mu_3\text{-}S)_4(\mu\text{-}S)_{12}(SPh)_4]^{6-}$ [29] or $[M^{II}_{10}(\mu_3\text{-}ESiMe_3)_4(\mu\text{-}X)_{12}\{E(SiMe_3)_3\}_4]$ ($M^{II}$ = Zn, Cd; E = P, As; X = Cl, Br, I).[30] However, in contrast to these compounds, the $[M_5Sn_5S_{20}]^{10-}$ units in **1**−**3** contain two types of metal atoms to become the first ternary aggregates of the T3-type structure. As with the quoted Cd/In/S anions and the $[B_{10}(S_{4/2})S_{16}]^{6-}$ or $[In_{10}(S_{4/2})S_{16}]^{6-}$ units in the binary open framework structures of $Ag_{10}[B_{10}S_{18}]$[31] or $(Me_2NH_2)_6[In_{10}S_{18}]$,[32] the anions in **1**−**3** do not covalently bind to an organic ligand shell at the surface but are stabilized by coordinative interactions within the alkali metal counterion aggregation.

The terminal bonds, $Sn-S_{term}$, are shorter by 0.044−0.054 (**1**), 0.042−0.046 (**2**), or 0.064−0.086 Å (**3**) than those of the bridging sulfide ligands Sn−($\mu$-S). Both types of Sn−S bonds are longer on average (to a maximum of +0.035 Å for $Sn-S_{term}$ or +0.058 Å for Sn−($\mu$-S)) than the respective ones in the discrete $[M_4Sn_4S_{17}]^{10-}$ anions.[14] This reflects the occurrence of harder and thus more tightly coordinating $Na^+$ ions instead of $K^+$ in the crystal lattice.

The differences between the M−($\mu$-S) and M−($\mu_3$-S) bond lengths within any one cluster ion in **1**, **2**, or **3** are not large. However, the M−($\mu$-S) distances are longer on average than the M−($\mu_3$-S) distances, and a similar observation was made with the $[M_4Sn_4S_{17}]^{10-}$ cluster anions that have Sn−($\mu$-S) bonds longer than the Sn−($\mu_4$-S) bonds.[14] The M−($\mu$-S) distances are again somewhat larger on average than those in the cited ternary anions (deviations of −0.013 to +0.052 Å). The values of the Zn−($\mu_3$-S) bonds in **1** lie within the range of those in the known complexes $(NMe_4)_4[Zn_{10}(\mu_3\text{-}S)_4(SPh)_{16}]$ (2.301−2.306 Å),[33] $[Zn_{10}(\mu_3\text{-}S)_4(\mu\text{-}SEt)_{12}(NC_7H_9)_4]$ (2.286−2.318 Å),[34] or $[Zn_{10}(\mu_4\text{-}S)(\mu_3\text{-}S)_6(SO_4)_3(py)_9]\cdot 3H_2O$ (2.267−2.359 Å),[35] which are the only further examples of structurally characterized clusters with "naked" $\mu_3$-S bridges between zinc atoms. The Co−($\mu_3$-S) distances in structurally related Co−S complexes vary strongly as a result of different bonding partners at the sulfur atoms (metal or C atom), varying coordination numbers, and different formal oxidation states. However, distances from tetracoordinate $Co^{II}$ centers to ($\mu_3$-S) or ($\mu$-SR) ligands were reported to be 2.276−2.371 Å,[37] a range that spans the observed Co−($\mu_3$-S) bond lengths in **2** and **3**.

In contrast to the complex counterion aggregates that were observed in the related M/Sn/Se compounds, the counterion networks in **1**−**3** are much less complicated because all of the $Na^+$ ions are octahedrally coordinated by solvent molecules or S ligands from the ternary anions. However, the O/S ratios of the coordination polyhedra $[NaO_{6-n}S_n]$ differ significantly when comparing **1** and **2** ($n$ = 0−2) on one hand and **3** ($n$ = 4−6) on the other hand. Consequently, the coordination spheres surrounding the anions in **1** and **2**, on one hand, and **3**, on the other, are dissimilar from each other and are thus described separately.


(26) Krebs, B. *Angew. Chem., Int. Ed. Engl.* **1983**, *22*, 113−134.
(27) Eichhöfer, A.; Fenske, D.; Pfistner, H.; Wunder, M. *Z. Anorg. Allg. Chem.* **1998**, *624*, 1909−1914.
(28) Behrens, S.; Bettenhausen, M.; Deveson, A. C.; Eichhöfer, A.; Fenske, D.; Lohde, A.; Woggon, U. *Angew. Chem., Int. Ed. Engl.* **1996**, *35*, 2215−2218.
(29) Krebs, B.; Henkel, G. *Angew. Chem., Int. Ed. Engl.* **1991**, *30*, 769−788.
(30) (a) Fuhr, O.; Fenske, D. *Z. Anorg. Allg. Chem.* **1999**, *625*, 1229−1236. (b) Eichhöfer, A.; Fenske, D.; Fuhr, O. *Z. Anorg. Allg. Chem.* **1997**, *623*, 762−768.
(31) Krebs, B.; Dierks, H. *Z. Anorg. Allg. Chem.* **1984**, *518*, 101−114.
(32) Cahill, C. L.; Ko, Y.; Parise, J. B. *Chem. Mater.* **1998**, *10*, 19−21.
(33) Dance, I. G.; Choy, A.; Scudder, M. L. *J. Am. Chem. Soc.* **1984**, *106*, 6285−6295.
(34) Nyman, M. D.; Hampden-Smith, M. J.; Duesler, E. N. *Inorg. Chem.* **1996**, *35*, 802−803.
(35) Ali, B.; Dance, I. G.; Craig, D. C.; Scudder, M. L. *J. Chem. Soc., Dalton Trans.* **1998**, 1661−1667.
(36) (a) Dance, I. G. *J. Am. Chem. Soc.* **1979**, *101*, 6264−6273. (b) Tremel, W.; Krebs, B.; Henkel, G. *Angew. Chem., Int. Ed. Engl.* **1984**, *23*, 634−635. (c) Wie, G.; Liu, H.; Huang, Z.; Kang, B. *J. Chem. Soc., Chem. Commun.* **1989**, 1839−1840. (d) Henkel, G.; Weissgraber, S. *Angew. Chem., Int. Ed. Engl.* **1992**, *31*, 1368−1369. (e) Cecconi, F.; Gilhardi, C. A.; Midollini, S.; Orlandini, A. *Polyhedron* **1986**, *5*, 2021−2031. (f) Barbaro, P.; Cecconi, F.; Gilhardi, C. A.; Midollini, S.; Orlandini, A.; de Biani, F. F.; Laschi, F.; Zanello, P. *J. Chem. Soc., Dalton Trans.* **1996**, 4337−4344. (g) Kang, B.-S.; Wen, T.-B.; Yu, X.-Y.; Zhang, H.-X.; Tong, Y.-X.; Su, C.-Y.; Chen, Z.-W.; Liu, H.-Q. *J. Cluster Sci.* **1999**, *10*, 429−443.
(37) For example, see: (a) Mattes, R.; Mühlenbrock, C.; Leeners, K.; Pyttel, C. *Z. Anorg. Allg. Chem.* **2004**, *630*, 722−729. (b) Kersting, B.; Siebert, D.; Volkmer, D.; Kolm, M. J.; Janiak, C. *Inorg. Chem.* **1999**, *38*, 3871−3882.

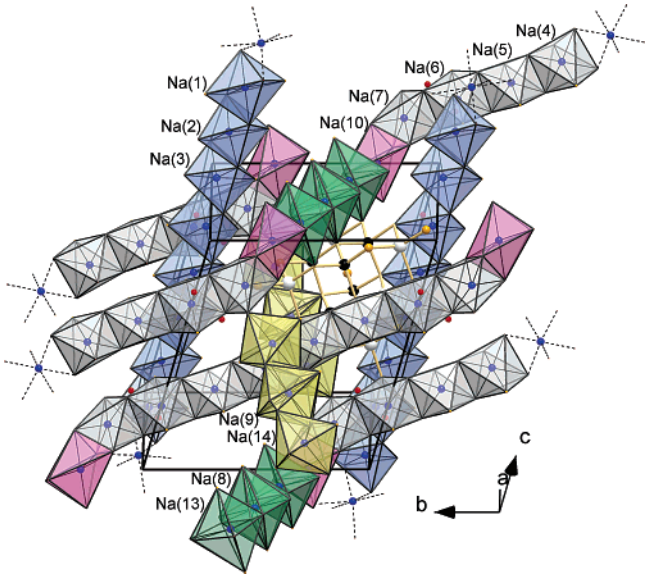


**Figure 2.** View of the crystal packing in **2**. Differently orientated domains of octahedral edge- or corner-sharing $[NaO_{6-n}S_n]$ units ($n = 0-2$) are represented by different colors (see text). Free water molecules are represented by their O atom (red). For clarity, only one of the two disordered orientations of the groups of three octahedra (yellow or green) is drawn in each case.

In the isotypic **1** and **2**, four domains of chains of differing lengths are formed by trans-edge or face sharing of the coordination octahedra around the $Na^+$ ions. Figure 2 shows a view of the crystal packing in **2** as an example, highlighting the domains by different colors: Na(1)−Na(3) (blue) produce an infinite chain parallel to the *c*-axis near $a = 1/2$ and $b = 0$. Na(4)−Na(7) (gray) are linked to give chains of eight octahedra, the ends of which share the opposing $\Delta_3$-face with further octahedra (Na(10), pink). These $[NaO_xS_y]_{10}$ aggregates are positioned in the *bc* plane of the unit cell. Cations Na(8) and Na(13) (green) as well as Na(9) and Na(14) (yellow) form sets of three octahedra that connect the longer chains around 1/2, 1/2, 0 (Na(8)) or 1/2, 1/2, 1/2 (Na(9)). Atoms Na(13) or Na(14) are only half occupied because of a statistical disorder of these short chains with another set of three octahedra, involving either Na(11) or Na(12) and their symmetry equivalents around Na(8) or Na(9), respectively. These two triplets of octahedra each follow one of two crossover directions, the second of which is omitted in Figure 2 for clarity. Additionally, two free water molecules are integrated in the lattice (O(51) and O(52) in **1** and **2**); they are each hydrogen bonded to two coordinated water molecules and two S atoms with tetrahedral geometries (O···S distances of 3.175(7)−3.406(11) Å in **1** and 3.135(7)−3.322(8) Å in **2** and O···O distances of 2.623(12)−3.016(9) Å in **1** and 2.700(14)−2.787(12) Å in **2**).

In the crystal structure of **3**, removal of most of the water molecules causes a rearrangement of the cluster anions within the crystal lattice. Figure 3 shows a comparison of both the crystal packing in **2** and **3**.

Upon changing from **2** to **3** by removal of 28 water molecules per formula unit, three distinct structural changes are observed. First, since nearly twice as many $Na^+$ ions are coordinated by the S ligands from a given anionic unit (28 $Na^+$ ions in **3** vs 17 in **2**), many interatomic distances are slightly longer within the cluster ion in **3** compared to those in **1** (c.f. Table 2). The differences amount to a maximum of 0.0046 Å for the Sn−($\mu$-S) bonds.

Second, the ternary anions approach each other more closely as a result of the greater number of S···Na···S contacts in **3** compared to the number in **2**. In the latter, only 13 $Na^+$ ions out of the 17 coordinated by each cluster form two Na···S contacts each, thus bridging to adjacent cluster anions; the remaining four $Na^+$ ions only interact with one S ligand and five water molecules each. In contrast, all 28 $Na^+$ ions that surround each ternary anion in **3** bridge to neighboring cluster anions; moreover, all show coordination by at least four S ligands, and most by five or six S ligands, and thus, by only two, one, or no $H_2O$ molecules. In this way, the $Na^+$ ions bridge between up to three Co/Sn/S anions at once so that the ternary anions in **3** are closer to the adjacent anionic units and show a smaller nearest S···S distance between two Co/Sn/S units than those in **2** (4.8 vs 5.9 Å).

Third, one observes a difference of the relative orientation of the Co/Sn/S units in **3** compared to that in **2**. In **2**, all the ternary T3-type anions have one of the large tetrahedral $(S_{term})_3$ faces orientated nearly parallel to the crystallographic *bc* plane, with the clusters as a whole pointing alternately above and below it. Such double layers of ternary anions arranged "up and down" with parallel orientation of one of their tetrahedral $(S_{term})_3$ faces, which run through the crystal parallel to *bc*, are also formed in **3**, but the $(S_{term})_3$ faces are now inclined by ca. 12.5° away from the *bc* plane. The closer approach of the cluster units in **3** might result in the pronounced metallic luster of the dehydrated quaternary phase, indicating some kind of inter-cluster interactions. To explore this, we are currently preparing experiments to check the metallic conductivity of this material.

**Optical Absorption Behavior of 1 and 2.** Figure 4 shows the absorption spectra of compounds **1** and **2** as suspensions in Nujol from 1100 to 250 nm, corresponding to an energy range of 1.1−5.0 eV.

The colorless crystals of **1** do not show any UV−vis absorption below 3 eV. The onset of absorption is observed at 377 nm (3.3 eV) which can be assigned to the lowest possible electronic excitation energy (i.e., the energy difference between the highest-occupied and lowest-unoccupied molecular orbitals of the cluster anions in the solid). For **2**, a sharp onset of absorption is observed at 940 nm (1.3 eV), again indicating the smallest possible excitation energy for charge-transfer processes in the compound. With decreasing wavelength, compound **2** shows significant absorption over the whole UV−vis range with several maxima at 833, 743, and 415 nm (1.5, 1.7, and 3.0 eV) and shoulders at 693, 463, and 387 nm (1.8, 2.7, and 3.2 eV) in accordance to its brownish black appearance. Only little is known about the absorption behavior of $Co^{II}S$-cluster complexes; however, the related compound $K_{10}[Co_4Sn_4S_{17}]$ shows an onset of absorption at 1.8 eV, consistent with its the somewhat smaller cluster size.[14b] The absorptions at higher energies are the result of d−d transitions and are consistent with the

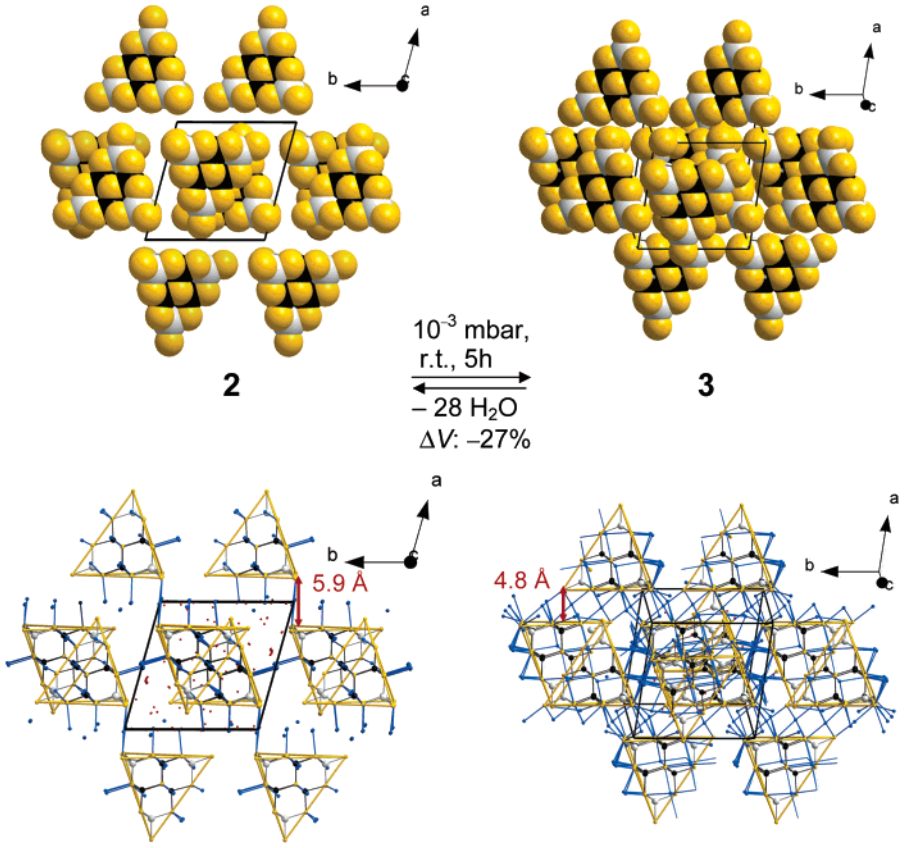


**Figure 3.** View of the crystal packing in **2** (left-hand side) and **3** (right-hand side) as space-filling models omitting $Na^+$ ions and $H_2O$ molecules (top) or as ball-stick representations (bottom). Co: black. Sn: light gray. S: yellow. Na: blue. O: red. Na···S interactions are given as blue sticks (bottom) to show the higher Na···S connectivity in **3** vs **2**. For clarity, Na···O interactions are not shown, and O atoms are only drawn in the unit cell. The tetrahedral shape of the T3-type Co/Sn/S clusters is emphasized by drawing the $S_{term}$···$S_{term}$ connecting lines (bold yellow).

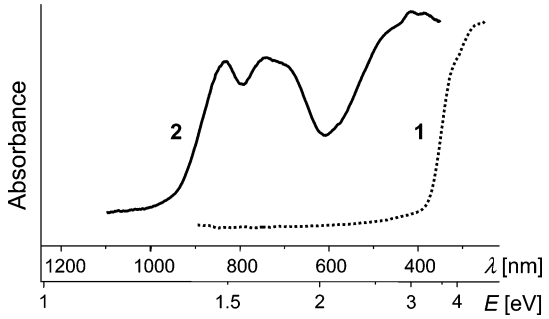


**Figure 4.** Absorption spectra of **1** (dotted) and **2** (solid).

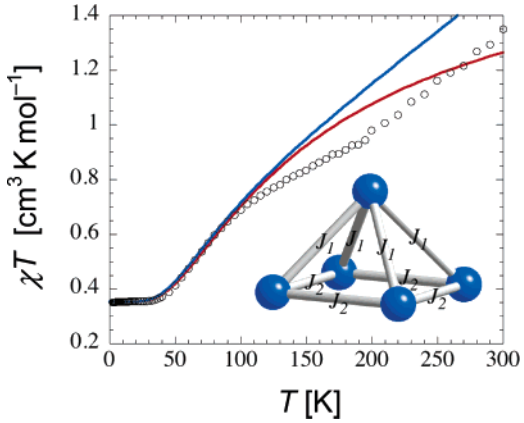


**Figure 5.** $\chi T$ vs $T$ plot of a polycrystalline sample of **3** (0.010 g) measured between 1.8 and 300 K at 1000 Oe. Solid blue and red lines correspond to the modeling approach developed in the text. The inset shows a simplified topology of the magnetic interactions between the five Co(II) centers.

complicated UV−vis spectra of previously reported molecular Co(II) complexes.[37]

**Magnetism of 3.** To investigate the magnetic behavior of the cobalt compound, we measured the magnetic susceptibility of a polycrystalline sample of **3**. The $\chi T$ vs $T$ plot is given in Figure 5.

Between 1.8 and 40 K, the $\chi T$ product is essentially constant at 0.35 $cm^3$ K $mol^{-1}$ in good agreement with an $S = 1/2$ ground state. As the temperature increases, the $\chi T$ product begins to increase in a nonlinear manner above 40 K. This unusual temperature dependence, observed in all the samples of **3** measured, reveals the presence of excited states that are successively populated with increasing temperature. This feature and the presence of a doublet ground state strongly suggest that significant antiferromagnetic interactions between $Co^{II}$ centers are present in the Co cluster. We attempted to model the magnetic susceptibility on the basis of the square-pyramidal arrangement of the tetrahedral $Co^{II}$ centers (see inset of Figure 5) which are bridged by $\mu_3$-S atoms. On the basis of the topology of the magnetic pathways, the magnetic susceptibility has been calculated using the MAGPACK program developed by Clemente-Juan and co-workers and the following Heisenberg Hamiltonian: $H = -2J_1[S_1(S_2 + S_3 + S_4 + S_5)] - 2J_2(S_2 + S_4)(S_3 + S_5)$.[38,39] With this approach and considering (i) only $S = 1/2$

spins (solid red line in Figure 5 with $J_1/k_B = J_2/k_B = -62(1)$ K) or (ii) one $S = 1/2$ (top spin of the pyramid, inset of Figure 5) and four $S = 3/2$ spins (solid blue line in Figure 5 with $J_1/k_B = -420(5)$ K and $J_2/k_B = -150(5)$ K), the susceptibility at lower temperatures (i.e., below 90 K) was well simulated with antiferromagnetic interactions between the spin carriers, as confirmed by DFT calculations ($T = 0$ K, see below). Nevertheless, we were not able to model, even qualitatively, the peculiar "S" shape observed on the $\chi T$ vs $T$ plot. This is not completely surprising considering that the effects of spin−orbit coupling and anisotropy have not been considered and that the symmetry of the $Co_5Sn$ cluster is lower than the idealized scheme displayed in the inset of Figure 5. Therefore, with five crystallographically independent $Co^{II}$ centers, up to eight different magnetic interactions must be taken into account in the model. In practice, this cannot be done without an over-parametrization of the model, and no attempt was made to reproduce the experimental data over the whole temperature range and to evaluate the antiferromagnetic interactions, quantitatively.

**Quantumchemical Investigations.** Density functional (DFT) methods were employed both to check the agreement of the experimentally determined structural parameters with the given sum formulas of **1**−**3** and to investigate the spin situation in the Co/Sn/S cluster anions in **2** and **3**. Anions $[Zn_5Sn_5S_{20}]^{10-}$ and $[Co_5Sn_5S_{20}]^{10-}$ were calculated within a simulated coordination sphere of 10 positive mirror charges, constructed using the COSMO model.[21] This method has proved to be both necessary and suitable for DFT calculations of highly charged ternary M/Sn/E anions.[13]

For M = Zn, a diamagnetic state ($S = 0$) was found, which is consistent with its colorless appearance. For $[Co_5Sn_5S_{20}]^{10-}$, various spin states are possible. One might think of total spins of $S = 15/2$ resulting from parallel spins at all five Co atoms (each of them contributing $S = 3/2$), of $S = 1/2$ (antiparallel spins with a remaining contribution of $S = 1/2$ from one of the five Co atoms), or of values between those mentioned above with $S = (2n + 1)/2$ ($n = 1-6$). Single-point DFT calculations were carried out for all of these spin states, starting with the high-spin case $S = 15/2$, and then successively lowering the number of unpaired electrons by 2 until $S = 1/2$ was reached. By this procedure, we found solutions with a positive gap between highest-occupied and lowest-unoccupied molecular orbitals, thus fulfilling the *aufbau* principle, for the cases $S = 15/2$, $S = 9/2$, $S = 3/2$, and $S = 1/2$. After the relaxation of the structure parameters for these four cases, the three states with antiparallel spins turned out to be 0.5−0.8 eV more stable than the $S = 15/2$ state; a more detailed discussion of the energetic sequence is not feasible because the effects of spin−orbit coupling are not included in the present scalar relativistic treatment. However, the existence of different spin states with relatively small energy differences was also observed in the experimental investigation of the temperature dependency of the magnetic susceptibility (Figure 5).

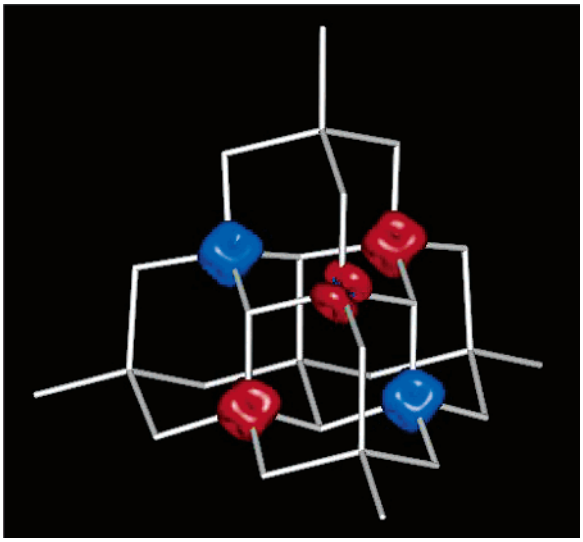

**Figure 6.** Plot of the spin density of the calculated $[Co_5Sn_5S_{20}]^{10-}$ anion with a calculated spin state of $S = 1/2$. Spin densities (i.e., difference of densities for α and $\beta$ spins) are drawn to 0.3 $e^-$ $Å^{-3}$.

**Table 3.** Distances (Å) and Angles (deg) for the Calculated $[M_5Sn_5S_{20}]^{10-}$ Anions[a]

| | $[Zn_5Sn_5S_{20}]^{10-}$ | $[Co_5Sn_5S_{20}]^{10-}$ |
|---|---|---|
| Sn−$S_{term}$ | 2.425−2.428 | 2.389−2.423 |
| Sn−($\mu$-S) | 2.422−2.454 | 2.435−2.574 |
| M−($\mu$-S) | 2.436−2.442 | 2.269−2.350 |
| M−($\mu_3$-S) | 2.339−2.344 | 2.187−2.336 |
| M···M ($O_h$ edges) | 3.795−3.716 | 3.640−3.847 |
| $S_{term}$−Sn−($\mu$-S) | 107.9−108.5 | 104.0−114.3 |
| ($\mu$-S)−Sn−($\mu$-S) | 110.4−110.8 | 106.8−112.4 |
| ($\mu$-S)−M−($\mu$-S) | 100.4−100.8 | 99.7−102.7 |
| ($\mu$-S)−M−($\mu_3$-S) | 108.2−108.4 | 100.4−115.9 |
| ($\mu_3$-S)−M−($\mu_3$-S) | 118.1−118.5 | 103.9−114.1 |
| M−($\mu$-S)−Sn | 103.7−104.0 | 102.7−109.3 |
| M−($\mu_3$-S)−M | 104.6−105.1 | 103.3−113.4 |

[a] M = Zn or Sn for **1** and M = Co or Sn for **2** and **3** in the case of the six core atoms.

Investigation of the spatial distribution of unpaired electrons (i.e., the difference of the electronic densities of α and $\beta$ electrons, "spin density") shows a clear localization at the Co atoms for all four cases; in Figure 6, the calculated spin density is plotted for the case $S = 1/2$.

Because of the localized character of the spin density, Mulliken population analyses for this quantity are expected to give reliable results. Indeed, for $S = 15/2$, $S = 9/2$, and $S = 3/2$, the number of unpaired of electrons per Co atom is 2.2−2.5, in reasonable agreement with to the expected value of 3 (for tetrahedrally surrounded $Co^{II}$ centers). For $S = 1/2$, we observed a significantly smaller number of unpaired electrons (1.4) for the Co center, which is at the corner of the cube opposite to the Sn atom (see Figure 6), together with 2.2−2.3 unpaired electrons, as before, at the four other Co atoms. This lower-spin situation is unprecedented to date but may serve to rationalize the observed magnetic behavior.

To confirm the compositions of **1** and **2**, we compared the structural parameters from the calculations on the anions with the experimental values. Table 3 summarizes the

(38) Kambe, K. *J. Phys. Soc. Jpn.* **1950**, *5*, 48.
(39) (a) Borrás-Almenar, J. J.; Clemente-Juan, J. M.; Coronado, E.; Tsukerblat, B. S. *Inorg. Chem.* **1999**, *38*, 6081−6088. (b) Borrás-Almenar, J. J; Clemente-Juan, J. M.; Coronado, E.; Tsukerblat, B. S. *J. Comput. Chem.* **2001**, *22*, 985−991.

distances for the calculated anions $[M_5Sn_5S_{20}]^{10-}$ (M = Co, Zn). For M = Co, the given ranges include the data from all optimized species.

Most calculated distances are somewhat greater than the observed values, as is often found with DFT (BP86) methods. Deviations from the experimental bond lengths are 0.03−0.07 Å for Sn−S in **1**, 0.02−0.17 Å for Sn−S in **2** or **3**, 0.01−0.08 Å for Zn−S, and −0.14−0 Å for Co−S. Angles deviate by ±2° around Sn in **1**, −2 to +1° around Sn in **2** or **3**, ±0 to −3° around Zn, −9 to +4° around Co, ±0 to −1° around S in **1**, and −2 to +5° around S in **2** or **3**.

## Conclusions

Reactions of $Na_4[SnS_4]$ with $ZnCl_2$ or $[Co(en)_3]X_3$ (X = Cl, Br) in water followed by layering with THF leads to the isolation of novel quaternary compounds, $[Na_{10}(H_2O)_{32}][Zn_5Sn(\mu_3\text{-}S)_4(SnS_4)_4]\cdot 2H_2O$ (**1**) and $[Na_{10}(H_2O)_{32}][Co_5Sn(\mu_3\text{-}S)_4(SnS_4)_4]\cdot 2H_2O$ (**2**), with unusual anionic subunits. The reactions that lead to the formation of **1** and **2** are, therefore, the first to prove, crystallographically, that there is a transfer of $[SnS_4]^{4-}$ anions into the coordination sphere of transition metal ions. By application of dynamic vacuum to compound **2**, single crystals of the partial dehydration product of **2**, $[Na_{10}(H_2O)_6][Co_5Sn(\mu_3\text{-}S)_4(SnS_4)_4]$ (**3**), were obtained. Compounds **1**−**3** were structurally characterized by single crystal X-ray diffraction, revealing the presence of a previously unknown type of ternary anion: a T3-type supertetrahedron consisting of Co (or Zn), Sn, and S atoms, the topology of which has previously only been observed with binary clusters of $d^{10}$ metal elements. Because of the presence of 10 $Na^+$ ions per formula unit, as was observed for all three phases, a fifth tin atom has to be assigned to an inner cluster position, being distributed over six positions together with five M atoms for the overall charge neutrality of the compounds. This has been confirmed by elemental analysis, by the reasonable thermal ellipsoids of the resulting Sn/M hybrid positions, by analysis of the structural parameters in comparison to related compounds, and by geometry optimization using DFT methods of respective $[M_5Sn_5S_{20}]^{10-}$ anions. Magnetic measurements of **3** and DFT investigations of the $[Co_5Sn_5S_{20}]^{10-}$ anion indicate antiferromagnetic coupling of the $\mu_3$-S-bridged $Co^{II}$ centers.

Future investigations are designated to concentrate on two topics: first, the exploration of the synthetic use of other chalcogenotetrelate salts as well as transition metal compounds for the formation and isolation of novel quaternary compounds, and second, a detailed investigation of the physical properties of these compounds, such as optical characteristics and magnetism, as shown for **1**−**3**. In this way, we might gain a deeper insight into the formation mechanisms and electronic situation in such quaternary phases with discrete ternary M/E′/E anions.

**Acknowledgment.** This work was financially supported by the state of Baden-Württemberg (Margarete von Wrangell habilitation fellowship for S.D.), the German Science Foundation (DFG), the Fonds der Chemischen Industrie, the Université de Bordeaux I, the CNRS, and the Conseil Regional d'Aquitaine. The authors are also grateful to J. M. Clemente-Juan for teaching and providing the MAGPACK package and to Dr. E. Matern for recording the NMR spectra. We thank Prof. D. Fenske for generous support of our research activities. Provision of computational resources by Prof. R. Ahlrichs and provision of analytical equipment by Prof. A. K. Powell are gratefully acknowledged.

**Supporting Information Available:** Crystallographic data files in CIF format. This material is available free of charge via the Internet at http://pubs.acs.org.

IC050466O